УДК 681.5:621.8.023 DOI: 10.18324/2077-5415-2023-2-23-29

Model of a mechatronic module of the ankle exoskeleton

T.S. Hussein[1a], O.V. Veselov [2b]

[1]Don State Technical University; 1, Gagarin Sq., Rostov-on-Don, Russia
[2]Vladimir State University; 87, Gorky St., Vladimir, Russia
[a]tsh19801980@gmail.com ,[b] 010848_j@mail.ru
[a]https://orcid.org/0000-0003-1325-0888, [b] https://orcid.org/0000-0002-2147-0218

Creation of special load transfer devices when a person carries a load through an external frame, namely, the exoskeleton, is a dynamically developing trend. The anatomical characteristics of the human body and the design of the mechanical device, form a biomechanical system. Therefore, the complexity of creating an exoskeleton, in addition to the design features, is related to the synchronization of the subsystems: mechanical, drive, and electronic. Various structures for constructing such systems are known. However, not all functions of the known devices are performed efficiently. The paper considers a model of a mechatronic module for controlling an ankle joint of the exoskeleton. The mechanical system is represented by a cylindrical frame, inside which there are compression and extension springs, a screw-nut transmission, by means of which the springs and a set of structural elements are moved. The movement is provided by means of a valve motor and a speed regulator based on the proportional integral regulation scheme. Three types of sensors are used in the system for qualitative control. An accelerometer, which controls the beginning and the process of exoskeleton movement in space. A force-moment sensor installed in the sole of the exoskeleton orthosis gives information about the contact of the orthosis with the movement surface, and a position sensor evaluates the location of the nut. The control is performed with the help of a microcontroller. The computational relationships of the mechanical system and the technique for tuning the speed controller to the modular optimum are given. Simulation in the Matlab environment with the use of Simulink and Sim Power System packages is performed. The structure and graphs of the model as a whole and its individual elements are given. The simulation of the mechatronic system according to the given structure confirms the correctness of the adopted solution and the efficiency of operation.

Keywords: exoskeleton, electromechanical system, actuators, interconnection, fuzzy controller.

Модель мехатронного модуля экзоскелета голеностопного сустава

Т.С. Хусейн[1a], О.В. Веселов[2b]

[1] Донской государственный технический университет, пл. Гагарина, 1, Ростов-на-Дону, Россия
[2] Владимирский государственный университет, ул. Горького, 87, Владимир, Россия
[a] tsh19801980@gmail.com, [b] 010848_j@mail.ru
[a] https://orcid.org/0000-0003-1325-0888, [b] https://orcid.org/0000-0002-2147-0218
Статья поступила 04.04.2023, принята 28.04.2023

Создание специальных устройств передачи нагрузки при переносе человеком груза через внешний каркас, экзоскелет, — динамично развивающееся направление. Анатомические характеристики человеческого тела и конструкция механического устройства образуют биомеханическую систему. Поэтому сложность создания экзоскелета, кроме конструктивных особенностей, связана с синхронизацией подсистем — механической, приводной и электронной. Известны различные структуры построения таких систем, однако не все функции известных устройств выполняются эффективно. В статье рассматривается модель мехатронного модуля управления экзоскелетом голеностопного сустава. Механическая система представлена цилиндрическим каркасом, внутри которого установлены пружины сжатия и растяжения, передача «винт – гайка», с помощью которой осуществляются перемещение пружин и набор конструктивных элементов. Перемещение обеспечивается с помощью вентильного двигателя и регулятора скорости, построенного по схеме пропорционально интегрального регулирования. Для качественного управления в системе используются три вида датчиков: акселерометр контролирует начало и процесс движения экзоскелета в пространстве; силомоментный датчик, установленный в подошве ортеза экзоскелета, дает информацию о контакте ортеза с поверхностью перемещения; датчик положения оценивает местоположение гайки. Управление осуществляется с использованием микроконтроллера. Приведены расчетные соотношения механической системы и методика настройки регулятора скорости на модульный оптимум. Выполнено моделирование в среде Matlab с использованием пакетов Simulink и Sim Power System. Приведены структура и графики работы модели в целом и отдельных ее элементов. Выполненное моделирование мехатронной системы по приведенной структуре подтверждает правильность принятого решения и эффективность функционирования.

Ключевые слова: экзоскелет; электромеханическая система; привод; мехатронный модуль; датчики.

Introduction. The changes currently taking place in the social environment, where human health is becoming a priority, require the manufacturer of goods and services to create effective approaches and means to improve the environment. It becomes important to develop technical means that provide comfortable living conditions in the event of

critical situations with human health [1–3]. One of the directions in industry and medicine is the development of exoskeletons that help a person compensate for the decrease in muscle strength during heavy physical exertion or injury [4–5].

Exoskeletons can be divided into four categories: for the back, for the legs, for the knee joint and for the hands. Each of the exoskeleton types can be used independently or be part of a design consisting of several types of exoskeletons. Exoskeletons provide a reduction in the load on different types of muscles in the workplace, which allows workers to perform various tasks. Move and fix relatively large parts, work with a mobile tool [6–8]. The listed exoskeletons can be used in production for a wide range of technological operations [9]. In medicine, exoskeletons are used for the rehabilitation of people with various diseases or injuries [10-11]. In sports, exoskeletons contribute to the formation of loads on various muscle groups [12]. The vast majority of exoskeletons are passive [13–15]. They have limited ability to control the transfer of force in the form of any function of changing the displacement [16–20]. Most passive exoskeletons using springs only partially provide unloading. In this case, muscle strength is used to stretch the spring. In many cases, it is required to completely unload the muscles. At present, much attention is paid to the development of active exoskeletons.

The aim of the research is to create a model of the mechatronic system of the ankle joint exoskeleton and to study the simulation model of movement using the exoskeleton. Consider an exoskeleton for the ankle joint built on the basis of a mechatronic module.

Mechatronic module. The block diagram of the mechatronic module is shown in Fig. 1. The frame of the lower limbs of the exoskeleton is structurally similar to the organoleptic features of the structure of the human body. The frame is a hollow cylinder, inside of which two springs are placed, with the help of which the movement is carried out. One of the springs works in tension and is located in the lower part of the cylinder, and the second in compression, installed in the upper part of the cylinder. A pair of screw-nut is installed between the springs, with the help of which the springs are moved. The springs are fixed on a rod connected to the platform on which the ankle support is attached. The mechatronic system and platform are attached to the orthosis. To move the nut, a brushless motor is used, which rotates the lead screw. Springs are attached to the nut, and when the nut moves, the springs are stretched and compressed. The speed of movement of the nut is carried out using a valve motor. The motor speed is controlled by a single-loop control system with a PI speed controller.

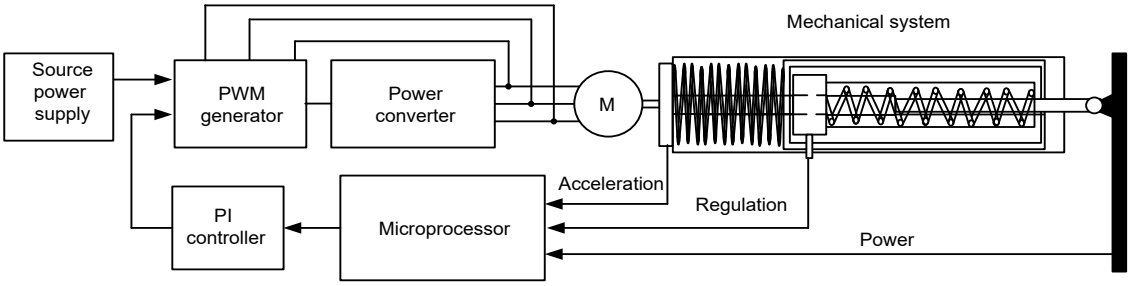

Fig. 1. Structural diagram of the mechatronic module

Process sensors are used to generate control signals for the module operation. The start of movement is controlled by an acceleration sensor installed at the top of the mechanism. The control of the interaction of the foot relative to the surface of movement is carried out by sensors of the force contact installed on the platform. The displacement is measured using a sensor, which is a linear potentiometer connected to the moving nut. The information coming from the sensors is processed by the microprocessor, which forms the speed value and the direction of movement. As a result of calculations of the mechanical system, the following data were obtained. Geometric parameters: spring diameter 20 mm, length 90 mm, lead screw length 100 mm, screw pitch 12 mm. Power parameters: elasticity 47.98 N for the compression spring and 70.21 N for the extension spring. The linear speed of movement is 0.1 m/s, the execution time of one step is 1.1 s. Let's select the engine and build the structure of the model. Choosing a non-contact DC motor (BDPT). The absence of a collector assembly greatly increases the reliability of operation and durability of use. The motor has the following main parameters: U_a = 24V ω = 418,67 rad/s, M = 0,06113 Nm, I_{max} = 5,4 A, R = 1,8 Ом, L_a = 2,6 10^{-3} GN, J = 0,0000024 Kg м^2.

Calculation of drive parameters. When synthesizing a speed controller, one has to simplify the mathematical description, replacing it with an equivalent DC motor. In this case, the equations that describe the BDPT will look like this:

$$u = R\,(Ts+1)\,i + p\,\omega_m\,\Phi_0,$$

$$M = pm\Phi_0/2i,$$

$$s\omega_m = (M - M_T)\,J^{-1},$$

$$s\theta_m = \omega_m,$$

Where u, i – motor voltage and current R, L, T, J, p Φ_0 – motor parameters, m = 3 – number of phases.

We calculate the parameters of the motor model according to the following relations:

$k_1 = 1/R_a$, – *motor factor;*

$k_м = pm\Phi_0/2$ *– structural mechanical constant;*

$k_2 = pm\Phi_0/2J$ *– rotor inertia*

$k_E = p\Phi_0$ *– structural electrical constant*

and summarize the data in table 1.

Table 1. Calculated parameters of the model

K_1	K_2	K_m	K_E	T_a	J	T_1	T_2
1/Om	1/Ams^2	Nm/A	Vs	s	Kgm^2	s	S
0,27	1522,8	0,0345	0,0366	0.0014	0.0000024	0.07	0,0012

These parameters are entered into the fields of the BLDT settings window when building the model.

In accordance with the equations in Fig. 2, the structure of the PMDC is shown. This structure is similar to the DPT structure.

The control transfer function can be represented as follows:

$$W(s) = \frac{\omega(s)}{U_a(s)} = \frac{{}^{1}/_{k_E}}{\frac{T_я}{k_1 k_2 k_E}s^2 + \frac{1}{k_1 k_2 k_E}s + 1},$$

where $k_1 = \frac{1}{R_a}$, $k_2 = \frac{k_m}{J}$.

We calculate the time constants by finding the roots of the characteristic equation:

$$s_{1,2} = 1/T_я \pm 1/T_я \sqrt{1 - 4T_a k_1 k_2 k_E},$$

$T_1 = -1/s_1$, $T_2 = -1/s_2$

The calculated values of the time constants are shown in table 1.

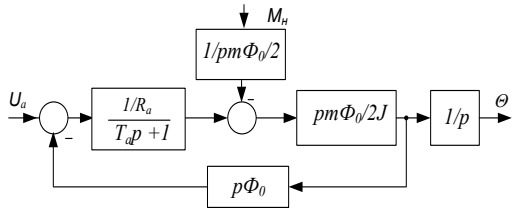

a

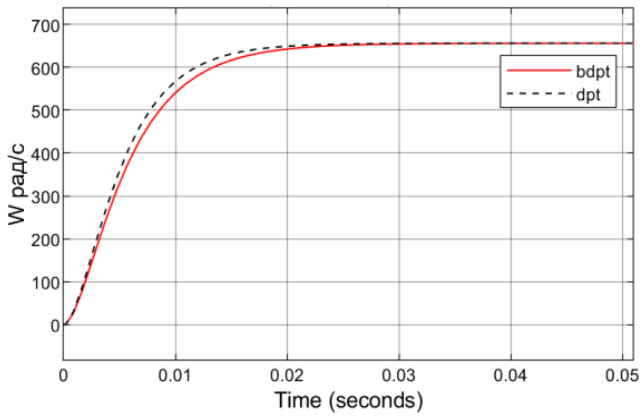

b

Fig. 2. Non-contact motor: *a* – model; *b* – graph of the transient process

Substituting the parameters from table 1 into the model and performing the simulation, we obtain a transient response. For comparison, the graph shows the transient response of a DC motor with the same parameters as for a non-contact DC motor. The steady value of the speed for both drives is the same, which makes it possible to use both models with equal success.

Calculation of the speed controller. The control transfer function can be represented as follows:

$$W(s) = \frac{\omega(s)}{U_a(s)} = \frac{{}^{1}/_{k_E}}{(T_1 s+1)(T_2 s+1)}.$$

Since the object is an aperiodic link with a transfer function for control:

$$W(s) = \frac{k_{PC}}{T_{PC} s + 1},$$

then a proportional-integral (PI) controller should be used. The transfer function of the controller has the form:

$W(s) = \frac{(T_2 s+1)k_p}{T_2 s}$.

In this case, the transfer function of an open system will be equal to:

$$W(s) = \frac{(T_2 s + 1)k_p \; k_{sr} k_{fb}}{T_2 s} \times \frac{{}^{1}/_{k_E}}{(T_1 s + 1)(T_2 s + 1)} =$$

$$= \frac{k_p \; k_{sr} k_{fb}/k_E}{(T_1 s+1)T_2 s}$$

The optimal modulus in such a system is achieved when:

$T_2 k_E / k_n \, k_p \, k_{fb} = 2T_1$,

where are the transfer coefficients of the proportional and integral parts of the regulator.

$k_p = T_2 k_E / 2T_1 \, k_n \, k_{fb}$, = 0,013

$k_u = k_p / T_2$. = 10,83

Let's build a model using the Simulink and SimPowerSystem software packages of the Matlab software environment. The peculiarity of the SimPowerSystem package is that it allows you to build a virtual model that is closest to the technical implementation. The model diagram (Fig. 3) includes a PMDC motor model, a power converter, switching circuits and a PI speed controller. Information about the main blocks of the model is given in table. 2.

Table 2. Blocks used in drive model

BDPT motor model

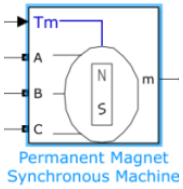

Stator phase resistance Rs (Ohm): 1.8

Stator phase inductance Ls (H) 2.6e-3

Machine constant

Specify: Flux linkage established by magnets (V.s)

Flux linkage: 0.014

Back EMF flat area (degrees): 120

Inertia, viscous damping, pole pairs, static friction [J(kg.m^2) F(N.m.s)

Initial conditions [wm(rad/s) thetam(deg) ia,ib(A)]: [0,0, 0,0]

Power Converter Model

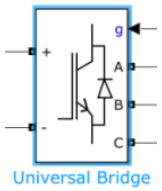

Parameters

Number of bridge arms: 3

Snubber resistance Rs (Ohms)

1e5

Snubber capacitance Cs (F)

inf

Power Electronic device IGBT / Diodes

Ron (Ohms)

1e-3

Switching circuit model (decoder)

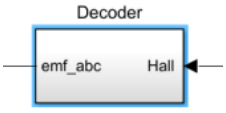

This module implements the following true table

ha	hb	hc	emf_a	emf_b	emf_c
0	0	0	0	0	0
0	0	1	0	-1	+1
0	1	0	-1	+1	0
0	1	1	-1	0	+1
1	0	0	+1	0	-1
1	0	1	+1	-1	0
1	1	0	0	+1	-1
1	1	1	0	0	0

Switching circuit model (setter)

This module implements the following true table

emf_a	emf_b	emf_c	Q1	Q2	Q3	Q4	Q5	Q6
0	0	0	0	0	0	0	0	0
0	-1	+1	0	0	0	1	1	0
-1	+1	0	0	1	1	0	0	0
-1	0	+1	0	1	0	0	1	0
+1	0	-1	1	0	0	0	0	1
+1	-1	0	1	0	0	1	0	0
0	+1	-1	0	0	1	0	0	1
0	0	0	0	0	0	0	0	0

Model PI speed controller

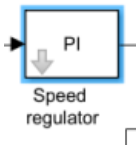

Parameters

Integral

15

Proportional:

.013

Minimum and maximum outputs:

[-500, 500]

The regulator parameters correspond to the calculated values.

The simulation results are shown in Fig. 4. The transition process time is 0.08 s, which is in good agreement with the time constraints for the execution time of one step equal to 1. 1s. The value of the set speed value exactly corresponds to the passport value of 4 000 rpm. (Fig. 4, *a*). The same results were obtained for the current in phase 5A

(upper graph in Fig. 4, *b*) and electromotive force 24 V (lower graph). The torque load, according to the passport values, leads to a speed drop within the specified limits.

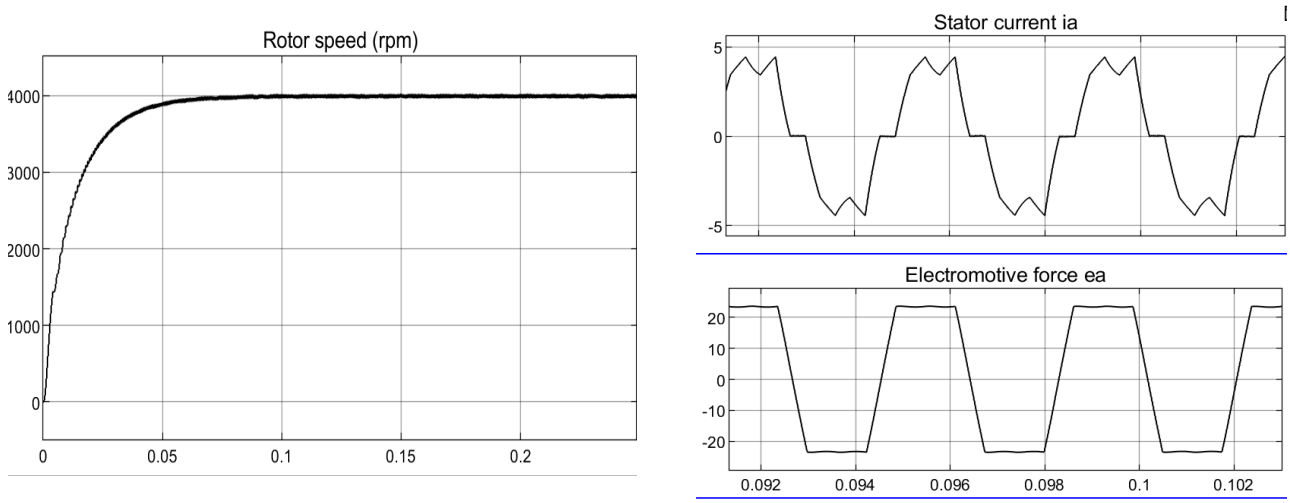

a *b*

Fig. 4. Drive simulation results: *a* – transient; *b* – current and voltage in phase

AThe current and voltage in phases B and C are similar to phase A. The drive provides a linear travel speed equal to: V = ρω= 0.8 m/s, which is slightly higher than the specified one. If necessary, this figure can be reduced by reducing the lead screw pitch.

Elements used in building a virtual model and settings are shown in table 2.

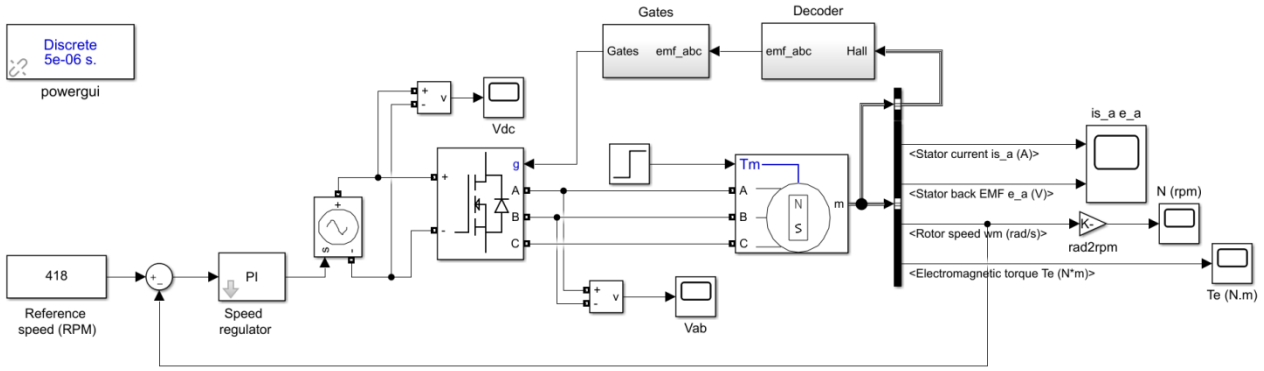

Fig. 3. Drive model

To simulate the algorithm for controlling the operation of the exoskeleton, it is necessary to integrate process sensors into the considered drive to generate control signals. There are three such sensors. The acceleration sensor determines the start of movement of the ankle exoskeleton. Force-torque sensor of the original design controls the contact of the foot with the moving surface. Position sensor, which determines the position of the screw-nut transmission nut.

The acceleration sensor is emulated with a sinusoidal signal. Indeed, with a uniform motion of the object, the real accelerometer signal is represented by a sinusoidal signal. However, in real conditions, the waveform is different from sinusoidal. This also applies to the torque sensor signal. For them, the amplitude and frequency are set commensurate with the pace of human movement. The displacement sensor signal is represented by a linear characteristic.

The simulation model of the system is shown in Fig. 5. In this case, to simplify the simulation procedure, the drive is presented as a DC drive model with the same parameters as in the model in Fig. 3.

In the figure, a drive containing a motor, a power converter (PWM) and a PI speed controller (PI speed controller) is highlighted in dark. Light background highlights sensor emulators: force (force sensor), acceleration (accelerometer) and position (position sensor). The sensor signals control the keys, which, upon reaching the set position, connect the speed reference signal, and the speed signal is transmitted at the moment when the signal level from the torque sensor decreases and Key1 is turned on.

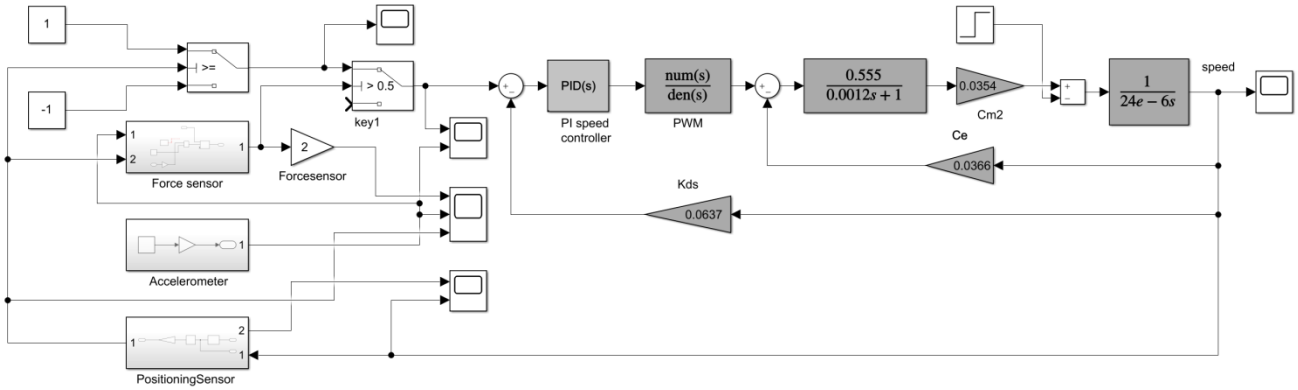

Fig. 5. Simulation model of the mechatronic module

The process begins with emulating the signal from the accelerometer and waiting for the signal from the torque sensor installed in the foot. The signal has a maximum value and decreases as the ankle rises. As soon as the signal level from this sensor decreases to a certain value, the key is activated, allowing the passage of the speed reference signal to the drive. At this point in time, the springs are deformed, helping to unload the muscles of the leg. The position of the deformable springs is controlled by a third sensor. After the transfer of the ankle, the latter is lowered and at this time the sign of the speed reference changes and the force-torque sensor is expected to operate. In studies, the drives are synchronized by introducing a delay in the control signal to one of the drives. The best solution in practical implementation will be the implementation of mutual control of drives. During the simulation, synchronization is carried out by a delay element for a time equal to the movement of one leg. The simulation used two identical models running in parallel.

Graphs simulating the steps of both legs are shown in Fig. 6.

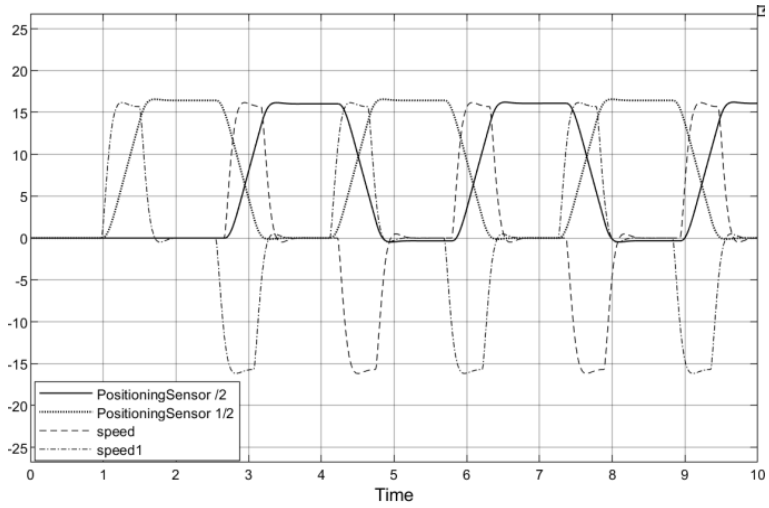

Fig. 6. Graph simulating steps

The graph shows changes in speed and movement in the drives of exoskeletons of both legs.

Conclusion. Modeling showed the fundamental possibility of constructing a mechatronic control module for the ankle joint exoskeleton. The given design parameters and a virtual drive model using a non-contact DC motor showed accurate results. Based on the data obtained, it is possible to implement the drive circuit without any changes. The simulation model demonstrated the correct implementation of the proposed drive control algorithm. At the same time, she set a number of tasks, such as the need for full-scale modeling and the choice of a microprocessor control device. It is essential to ensure interconnected control of drives, if the initiator (accelerometer) of the start of movement does not provide reliable control.

References

1. YAcun S.F., Savin S.I., Emel'yanova O.V., YAcun A.S., Turlapov R.N. Exoskeletons: analysis of structures, principles of creation, basics of modeling: monogr. Kursk, 2015. 179 p.
2. Egorov A.D. Mechanics and design of robots. M.: STANKIN, 1997. 510 p.
3. Bobyr' M.V. Theoretical foundations for constructing automated process control systems based on fuzzy logic. Staryj Oskol: Tonkie naukoemkie tekhnologii, 2019. 234 p.
4. Lukinov A.P. Design of mechatronic and robotic devices. SPb.: Lan', 2012. 606 p.
5. Krejg Dzhon. Introduction to robotics. Mechanics and management. M., Izhevsk: ANO Izhevskij in-t komp'yuternyh issledovanij, 2013. 543 p.

6. Mashkov K.YU., Rubcov V.I., Rubcov I.V. The composition and characteristics of mobile ro-bots. M.: Izd-vo MGTU im. Baumana, 2014. 175 p.
7. Musalimov V.M., Zamoruev G.B., Kalapyshina I.I., Perechesova A.D., Nuzhdin K.A. Modeling of mechatronic systems in the MATLAB environment (Simulink / SimMechanics). SPb.: NIU ITMO, 2013. 114 p.
8. Syreckij G.A. Systems Modeling. Part 2. Intelligent systems. Novosibirsk: NGTU, 2010. 80 p.
9. Minchala L.I., Astudillo-Salinas F., Palacio-Baus K., Vazquez-Rodas A. Mechatronic design of a lower limb exoskeleton. Mechatronic Systems in Engineering: Design, Control and Applications, 2017. P. 111-134.
10. Choi J., Park K.W., Park J., Lee D.H., Song E., Na B., Jeon S., Kim T., Choi H., Woo H., Lee J.H. The history and future of the walk ON suit: A powered exoskeleton for people with disabilities. IEEE Industrial Electronics Magazine, 2021. V. 16 (4). P. 16-28.
11. Yao S., Zhuang Y., Li Z., Song R. Adaptive admittance control for an ankle exoskeleton using an EMG-driven musculoskeletal model. Frontiers in neurorobotics, 2018. V. 12. P. 16.
12. Ao D., Song R., Gao J. Movement performance of human-robot cooperation control based on EMG-driven hill-type and proportional models for an ankle power-assist exoskeleton robot. IEEE Transactions on Neural Systems and Rehabilitation Engineering, 2016. V. 25 (8). P. 1125-1134.
13. Bougrinat Y., Achiche S., Raison M. Design and development of a lightweight ankle exoskeleton for human walking augmentation. Mechatronics, 2019. V. 64. P. 102297.
14. Zhu Y., Wu Q., Chen B., Zhao Z. Design and voluntary control of variable stiffness exoskeleton based on semg driven model. IEEE Robotics and Automation Letters, 2022. V. 7 (2). P. 5787-5794.
15. He Y., Liu J., Li F., Cao W., Wu X. Design and analysis of a lightweight lower extremity exoskeleton with novel compliant ankle joints. Technology and Health Care, 2022. V. 30 (4). P. 881-894.
16. Kuan J.Y., Pasch K.A., Herr H.M. A high-performance cable-drive module for the development of wearable devices. IEEE/ASME Transactions on mechatronics, 2018. V. 23 (3). P. 1238-1248.
17. Kuan J.Y., Pasch K.A., Herr H.M. A high-performance cable-drive module for the development of wearable devices. IEEE/ASME Transactions on mechatronics, 2018. V. 23 (3). P. 1238-1248.
18. Shi Y., Guo M., Wang R., Xia D., Luo X., Ji X., Yang Y. August. Modeling and Synergetic Simulation of a Lower Limb Exoskeleton Robot With the Human Subject. IEEE International Conference on Mechatronics and Automation, 2022. P. 1493-1498.
19. Bishe S.S.P.A., Nguyen T., Fang Y., Lerner Z.F. Adaptive ankle exoskeleton control: Validation across diverse walking conditions. IEEE Transactions on Medical Robotics and Bionics, 2021. V. 3 (3). P. 801-812.
20. Hussejn T.S., Izyumov A.I. Microprocessor system for measuring pressure between orthosis and foot // Systems. Methods. Technologies. 2023. № 1 (57). P. 80-86.

Литература

1. Яцун С.Ф., Савин С.И., Емельянова О.В., Яцун А.С., Турлапов Р.Н. Экзоскелеты: анализ конструкций, принципы создания, основы моделирования: моногр. Курск, 2015. 179 с.
2. Егоров А.Д. Механика и конструирование роботов. М.: СТАНКИН, 1997. 510 с.
3. Бобырь М.В. Теоретические основы построения автоматизированных систем управления технологическими процессами на основе нечеткой логики. Старый Оскол: Тонкие наукоемкие технологии, 2019. 234 с.
4. Лукинов А.П. Проектирование мехатронных и робототехнических устройств. СПб.: Лань, 2012. 606 с.
5. Крейг Джон. Введение в робототехнику. Механика и управление. М., Ижевск: АНО Ижевский ин-т компьютерных исследований, 2013. 543 с.
6. Машков К.Ю., Рубцов В.И., Рубцов И.В. Состав и характеристики мобильных роботов. М.: Изд-во МГТУ им. Баумана, 2014. 175 с.
7. Мусалимов В.М., Заморуев Г.Б., Калапышина И.И., Перечесова А.Д., Нуждин К.А. Моделирование мехатронных систем в среде MATLAB (Simulink / SimMechanics). СПб.: НИУ ИТМО, 2013. 114 с.
8. Сырецкий Г.А. Моделирование систем. Часть 2. Интеллектуальные системы. Новосибирск: НГТУ, 2010. 80 с.
9. Minchala L.I., Astudillo-Salinas F., Palacio-Baus K., Vazquez-Rodas A. Mechatronic design of a lower limb exoskeleton. Mechatronic Systems in Engineering: Design, Control and Applications, 2017. P. 111-134.
10. Choi J., Park K.W., Park J., Lee D.H., Song E., Na B., Jeon S., Kim T., Choi H., Woo H., Lee J.H. The history and future of the walk ON suit: A powered exoskeleton for people with disabilities. IEEE Industrial Electronics Magazine, 2021. V. 16 (4). P. 16-28.
11. Yao S., Zhuang Y., Li Z., Song R. Adaptive admittance control for an ankle exoskeleton using an EMG-driven musculoskeletal model. Frontiers in neurorobotics, 2018. V. 12. P. 16.
12. Ao D., Song R., Gao J. Movement performance of human-robot cooperation control based on EMG-driven hill-type and proportional models for an ankle power-assist exoskeleton robot. IEEE Transactions on Neural Systems and Rehabilitation Engineering, 2016. V. 25 (8). P. 1125-1134.
13. Bougrinat Y., Achiche S., Raison M. Design and development of a lightweight ankle exoskeleton for human walking augmentation. Mechatronics, 2019. V. 64. P. 102297.
14. Zhu Y., Wu Q., Chen B., Zhao Z. Design and voluntary control of variable stiffness exoskeleton based on semg driven model. IEEE Robotics and Automation Letters, 2022. V. 7 (2). P. 5787-5794.
15. He Y., Liu J., Li F., Cao W., Wu X. Design and analysis of a lightweight lower extremity exoskeleton with novel compliant ankle joints. Technology and Health Care, 2022. V. 30 (4). P. 881-894.
16. Kuan J.Y., Pasch K.A., Herr H.M. A high-performance cable-drive module for the development of wearable devices. IEEE/ASME Transactions on mechatronics, 2018. V. 23 (3). P. 1238-1248.
17. Kuan J.Y., Pasch K.A., Herr H.M. A high-performance cable-drive module for the development of wearable devices. IEEE/ASME Transactions on mechatronics, 2018. V. 23 (3). P. 1238-1248.
18. Shi Y., Guo M., Wang R., Xia D., Luo X., Ji X., Yang Y. August. Modeling and Synergetic Simulation of a Lower Limb Exoskeleton Robot With the Human Subject. IEEE International Conference on Mechatronics and Automation, 2022. P. 1493-1498.
19. Bishe S.S.P.A., Nguyen T., Fang Y., Lerner Z.F. Adaptive ankle exoskeleton control: Validation across diverse walking conditions. IEEE Transactions on Medical Robotics and Bionics, 2021. V. 3 (3). P. 801-812.
20. Хуссейн Т.С., Изюмов А.И. Микропроцессорная система измерения давления между ортезом и стопой // Системы. Методы. Технологии. 2023. № 1 (57). P. 80-86.